Int J Adv Manuf Technol (2017) 89:847–856
DOI 10.1007/s00170-016-9151-x

ORIGINAL ARTICLE

Rotary ultrasonic face grinding of carbon fiber reinforced plastic (CFRP): a study on cutting force model

Shuliang Liu[1] · **Tao Chen**[1] · **Chaoqun Wu**[1]

Received: 5 April 2016 / Accepted: 4 July 2016 / Published online: 12 July 2016

Abstract Carbon fiber reinforced plastic (CFRP) offers excellent mechanical properties, such as high strength, light weight, which makes it widely used in aerospace, transportation, machineries, and industrial applications. However, because of its anisotropic mechanical properties, high hardness, high strength, and poor thermal conductivity, the traditional processing methods are gradually unable to meet the processing needs. Except delamination, glitches, and tearing during processing, there are also other defects, like severe tool wear, larger cutting force, and higher cutting temperature, which make the tool life shortened. The machinability of CFRP materials using conventional machining (CM) techniques has seen a limited improvement over the years. Rotary ultrasonic machining (RUM) is an advanced machining process, which has shown to have specific advantages especially in the machining of CFRP. Many experimental investigations on cutting force in RUM of CFRP have been reported. However, in the literature, there are no reports on the development of a cutting force model for flat surface rotary ultrasonic machining, i.e., rotary ultrasonic face grinding (RUFG). In order to reveal the mechanism of grinding force reduction in RUFG of CFRP, based on material properties of CFRP, the brittle fracture theory approach was adopted and a cutting force model was developed for CFRP in RUFG process. The experiments were carried out and found the affect of the input variables for the cutting force in RUFG. The results were analyzed and discussed. The trends of predicted effects of input variables on cutting force agree well with the trends determined experimentally. Compared with the experimental results, the developed cutting force model was regarded as reasonable.

Keywords Carbon fiber reinforced plastic (CFRP) · Rotary ultrasonic machining (RUM) · Face grinding · Cutting force · Material removal mechanism

1 Introduction

Carbon fiber reinforced plastic (CFRP) composites are a class of extremely strong and light weight materials. The use of CFRP becomes more attractive today in various industrial sectors such as aerospace, naval, transportation, and machineries. This is due to their excellent mechanical properties (strength, stiffness, light weight, etc.) and fatigue resistance [1, 2]. However, machining of CFRP is considerably more difficult than machining of conventional metals for the reason of the obviously different material properties (high hardness, high strength, and poor thermal conductivity). Moreover, CFRP is inhomogeneous and an anisotropic composite material. Generally, conventional machining (CM) of CFRP encountered many problems such as delamination, splintering, burr, short tool life, low machining precision, and low surface quality [3–7]. In addition, high processing cost and low processing efficiency are main problems which hindered the applications of such materials. It is necessary to develop precise machining technology to raise working efficiency and improve surface quality.

Ultrasonic vibration machining (UVM) is a nontraditional machining process which is a hybrid process that combines

✉ Tao Chen
chent29@whut.edu.cn

[1] School of Mechanical and Electronic Engineering, Wuhan University of Technology, Wuhan, Hubei Province 430070, China

material removal mechanisms of grinding and ultrasonic machining [8, 9]. The cutting tool can oscillate at high frequency (typically 20 kHz) while being fed towards the workpiece. Since the introduction of ultrasonic vibration, many benefits can be obtained such as: changing the material removal mechanism, reducing the cutting force and the friction between the tool and the workpiece, reducing the cutting temperature, improving tool life and the precision and quality, enhancing the cutting capacity of the tools, thus effectively improve material removal rate [10, 11].

Several researchers have studied the effect of such vibrations assisted techniques to machine these difficult-to-cut materials. Qin et al. [12] presented a physics-based predictive model of cutting force in the ultrasonic vibration assisted grinding (UVAG) of Ti to predict the influences of input variables on cutting force. This model can serve as a foundation for development of cutting force models in UVAG of other materials (such as ceramics and stainless steels). But it is not suitable for CFRP materials. Liu et al. [13] developed a rotary ultrasonic drilling force model based on the brittle fracture theory. The shape of the diamond grit was assumed octahedron, and brittle fracture was assumed the primary mechanism of material removal in rotary ultrasonic machining (RUM) of brittle materials. The model can predict relationships between cutting force and input variables. Cong et al. [14] developed a mechanistic predictive model for cutting force in RUM of CFRP. It was found that material removal mechanism in RUM of CFRP can be studied using the indentation brittle fracture mechanics. CFRP can be treated as an equivalent homogeneous material to obtain the mechanical properties of CFRP from its components. Wang et al. [15] presented a mathematical model for system matching in ultrasonic assisted grinding (UAG) of brittle materials to reveal the mechanism of grinding force reduction and grinding quality improvement. The advantages of UAG processing brittle materials were pointed out in theory (such as grinding force reduction, the decrease of surface roughness). The developed models can predict influences of input variables on grinding force and workpiece surface topography. Hu and Zhang [16, 17] investigated the grinding performance of epoxy matrix composites reinforced by unidirectional and multidirectional carbon fibers. Compared with the unidirectional CFRP composites, the grinding forces for the multidirectional composites increase nearly linearly with raising the grinding depth. The chips produced showed a mixture of fine powder and broken fibers of various lengths, for the unidirectional fiber-reinforced composites the geometry of chips was mainly dependent on the fiber orientations.

In general, the previous study on RUFG of CFRP materials is rare. It is necessary to develop a cutting force model and to find the relationship between cutting force and its significant parameters. This paper presented a mathematical model for cutting force in RUFG of CFRP. Afterwards, using this developed model, it predicts effects of input variables including spindle speed, cutting depth, feed rate, and grit size on cutting force. Finally, these predicted effects are compared with the experimental results.

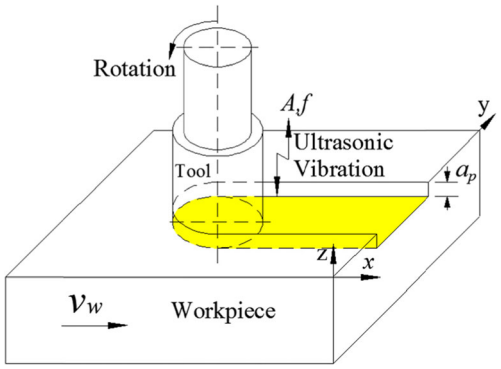

Fig. 1 Illustration of the rotary ultrasonic face grinding process

2 The kinematics analysis of rotary ultrasonic face grinding (RUFG)

2.1 The grain trajectory model of single abrasive

In RUFG, abrasive grain movement relative to the workpiece can be considered as hybrid motions including feed motion in the x direction, rotational circular motion, and sinusoidal motion in the z direction, as illustrated in Fig. 1.

Based on the RUFG kinematics analysis, we establish the single abrasive grain trajectory model:

$$x = v_w t + R_i \cos\frac{\pi}{30} n_s t \tag{1}$$

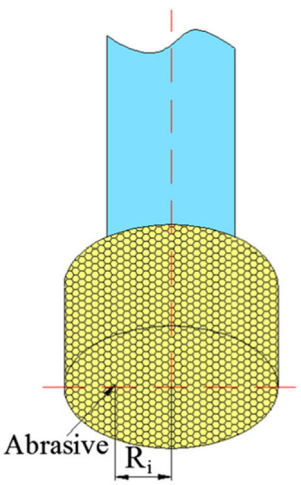

Fig. 2 Illustration of abrasive grain distribution

$$y = R_i \sin\frac{\pi}{30} n_s t \tag{2}$$

$$z = A\sin(2\pi ft + \varphi_0) \tag{3}$$

Where v_w is the workpiece feed speed (mm/min); R_i is the rotation radius of arbitrary abrasive grain i shown in the Fig. 2; n_s is the spindle speed (n/min, rpm); A is ultrasonic amplitude; and f is ultrasonic frequency; φ_0 is ultrasonic vibration initial phase.

Figure 3 shows the trajectory of single abrasive grain in RUFG. The initial values of the parameters were as follows: $v_w = 300$ mm/min, $R = 4$ mm, $n_s = 2000$ rpm, $A = 0.01$ mm, and $f = 20$ KHz.

According to the above equations, the velocity model of arbitrary single abrasive grain can be described as:

$$V_x = v_w - \frac{\pi}{30} n_s R_i \sin\frac{\pi}{30} n_s t \tag{4}$$

$$V_y = \frac{\pi}{30} n_s R_i \cos\frac{\pi}{30} n_s t \tag{5}$$

$$V_z = 2\pi fA\cos(2\pi ft + \varphi_0) \tag{6}$$

Assume the ultrasonic vibration initial phase $\varphi_0 = 0$, the trajectory length of arbitrary single grain contact with material during one cycle of ultrasonic vibration can be defined as follows:

$$L = \int \sqrt{V_x^2 + V_y^2 + V_z^2}\,dt = \int_0^{\Delta t} \sqrt{\left(v_w - \frac{\pi}{30} n_s R_i \sin\frac{\pi}{30} n_s t\right)^2 + \left(\frac{\pi}{30} n_s R_i \cos\frac{\pi}{30} n_s t\right)^2 + (2\pi fA\cos(2\pi ft + \varphi_0))^2}\,dt \tag{7}$$

For simplification, average radius $\bar{R}$ was used instead of R_i. Therefore, the average trajectory length of single abrasive grain can be defined as follows:

$$L = \int_0^{\Delta t} \sqrt{\left(v_w - \frac{\pi}{30} n_s \bar{\ } \sin\frac{\pi}{30} n_s t\right)^2 + \left(\frac{\pi}{30} n_s R \cos\frac{\pi}{30} n_s t\right)^2 + (2\pi fA\cos(2\pi ft + \varphi_0))^2}\,dt \tag{8}$$

Wherein $\bar{R}$ can be calculated as:

$$\bar{R} = \frac{R}{2} = \frac{D}{4} \tag{9}$$

2.2 Relationship between maximum penetration depth and cutting force

Due to the presence of ultrasonic vibration, the abrasive grain on the end face of the grinding unit is not in continuous contact with the workpiece. The certain period of time that the diamond particle effectively processes the workpiece surface in a single ultrasonic vibration cycle is called the effective cutting time Δt. Assume the maximum penetration depth of abrasive grain is δ. Δt can be accurately calculated as:

$$\Delta t = \frac{1}{\pi f}\left[\frac{\pi}{2} - \arcsin\left(1 - \frac{\delta}{A}\right)\right] \tag{10}$$

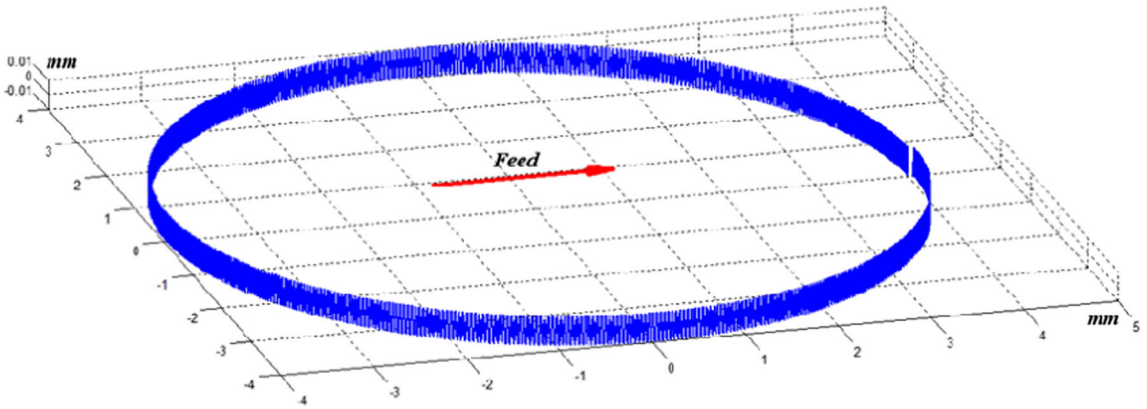

Fig. 3 Trajectory of single abrasive grain in RUFG

Applying the energy conservation theorem, then

$$I = \int_{\text{cycle}} F_{\text{i}}\, dt \approx F_{\text{i}} \Delta \text{t} \tag{11}$$

Where F_{i} is maximum impact force between tool and workpiece. The impulse I for one ultrasonic vibration cycle can also be expressed as:

$$I = \frac{F}{f} \tag{12}$$

Where F is the cutting force measured during the experiments in RUFG of CFRP.

By comparing Eq. (11) with Eq. (12), we can get

$$F = f F_{\text{i}} \Delta \text{t} \tag{13}$$

The indentation depth of abrasive grain into workpiece can be calculated by [18]:

$$\delta = \left[\frac{9}{16} \frac{\left(F_{\text{i}}/n\right)^2}{d/2} \left(\frac{1-\nu^2}{E}\right)^2 \right]^{1/3} \tag{14}$$

Where, E and v are the equivalent elastic modulus and Poisson's ratio of CFRP, respectively, which will be explained in Section 3.2; d is the size (diameter) of abrasive grains; n is the number of active abrasive grains on the end face of cutting tool. It can be determined by [13]:

$$n = \left(\frac{6 \times 0.88 \times 10^{-3}}{\pi d^3 \rho} \frac{C_{\text{a}}}{100} \right)^{2/3} A_0 \tag{15}$$

Where, C_{a} is the abrasive concentration; ρ is the density of abrasive material, $\rho = 3521\ \text{kg} \cdot \text{m}^{-3}$ for diamond; A_0 is the area of the cutting tool end face, $A_0 = \pi D^2/4$.

From Eq. (14), the maximum impact force between tool and workpiece can be expressed as:

$$F_{\text{i}} = \frac{\left(8d\delta^3\right)^{1/2} nE}{3(1-\nu^2)} \tag{16}$$

To simplify the numerical computation, we simplify the equation for the effective cutting time Δt as

$$\Delta \text{t} = \frac{\delta}{2Af} \tag{17}$$

From Eqs. (12), (16), and (17), the relationship between indentation depth of abrasive grain and cutting force was expressed as:

$$\delta = \sqrt[5/2]{\frac{3A(1-\nu^2)F}{(2d)^{1/2} nE}} \tag{18}$$

By substituting Eq. (18) in Eq. (17), the effective cutting time Δt can be expressed as:

$$\Delta \text{t} = \sqrt[5/2]{\frac{3(1-\nu^2)F}{8\left(f^5 A^3 d\right)^{1/2} nE}} \tag{19}$$

3 RUFG material removal rate and grinding force modeling

3.1 Assumptions in model development

1) Workpiece material is an ideally brittle material;
2) Fibers are continuous distribution and parallel to each other;
3) The bond between the fibers and matrix is perfect;
4) Fiber and matrix follow Hooke's law of linear elasticity;
5) The elastic modulus and diameter of fibers are uniform, and the same amount of space between the fibers;
6) The workpiece material without voids and cavities.

3.2 Elastic modulus and Poisson's ratio of CFRP

As all known, CFRP is clearly anisotropic. The value of a property varies with the direction along which it is measured. In the machining process, when the machining load is applied to different plane, the elastic modulus and Poisson's ratio of CFRP in different direction of the fibers should be used in model development. In detail, when the machining load is applied in the direction perpendicular to the "1" direction (Fig. 4), the elastic modulus and Poisson's ratio of CFRP in the longitudinal direction of the fibers should be used in model development. When the machining load is applied in the "3" direction, the elastic modulus and Poisson's ratio of CFRP in the transverse direction of the fibers should be used in model development.

The most successful application is the prediction of the stiffness parallel to the fibers, i.e., the longitudinal stiffness or modulus. According to the Rule or Law of Mixtures, the elastic modulus of CFRP in the longitudinal direction (E_{11}) of the fibers is [19] as follows:

$$E_{11} = E_{\text{f}} V_{\text{f}} + E_{\text{m}} V_{\text{m}} \tag{20}$$

Where, V_f and V_m are the volume fraction of the fiber and matrix in CFRP, respectively. E_f and E_m are the elastic modulus of fiber and matrix material in CFRP, respectively.

The fiber volume fraction is one of the main parameters in the determination of CFRP's mechanical properties. Generally, fiber volume fraction is calculated as:

$$V_f = \frac{w_f \rho_m}{w_f \rho_m + w_m \rho_f} = \frac{w_f \Big/ \rho_f}{w_f \Big/ \rho_f + w_m \Big/ \rho_m} = \frac{v_f}{v_f + v_m} \quad (21)$$

$$V_m = \frac{w_m \rho_f}{w_f \rho_m + w_m \rho_f} = \frac{w_m \Big/ \rho_m}{w_f \Big/ \rho_f + w_m \Big/ \rho_m} = \frac{v_m}{v_f + v_m} \quad (22)$$

Where, w_f and w_m are the weight of fibers and matrix, respectively. ρ_f and ρ_m are the density of fibers and matrix, respectively. v_f and v_m are the volume of fibers and matrix, respectively.

The corresponding expression for the transverse modulus of the composite is as follows:

$$\frac{1}{E_{22}} = \frac{V_f}{E_f} + \frac{V_m}{E_m} \rightarrow E_{22} = \frac{E_f E_m}{E_m V_f + E_f V_m} \quad (23)$$

It is usual to assume that E_f is the longitudinal value, if only because the transverse fiber modulus is extremely difficult to determine. This assumption will only be correct for isotropic fibers.

The longitudinal modulus model serves to provide a prediction for the major Poisson's ratio. The resulting expression is as follows:

$$\nu_{12} = \nu_f V_f + \nu_m V_m \quad (24)$$

There is a relationship between elastic modulus and Poisson's ratio in different directions.

$$\frac{\nu_{12}}{E_{11}} = \frac{\nu_{21}}{E_{22}} \quad (25)$$

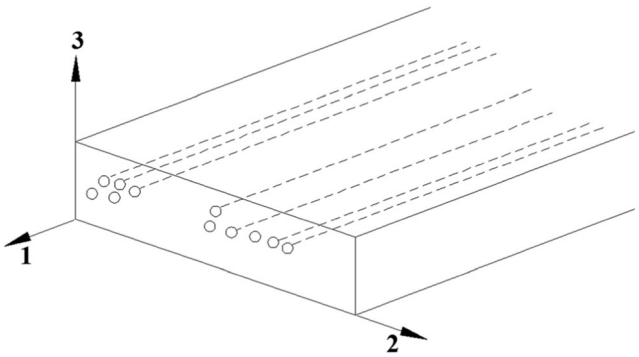

Fig. 4 Orientation of principal material axes

In this case, the Poisson's ratio in the transverse direction can be calculated by the following:

$$\nu_{21} = \nu_{12} \frac{E_{22}}{E_{11}} \quad (26)$$

3.3 Material removal volume by one abrasive grain

This article assumes that material removal mechanism in RUFG of carbon fiber composites is considered to follow brittle failure mechanism. Domestic and foreign scholars [10, 13, 15, 20, 21] have done a lot of research on the brittle fracture failure mechanism. Brittle material is applied in indenter under load and will have a central crack formed on both sides of expanding to a lateral crack and transverse cracks; transverse cracks in the material to be removed eventually peel off. In this case, the material removal is controlled by the cutting and abrasive track surface crack in the ground surface. The material removal volume processed by one abrasive grain during a single vibration cycle can be expressed as:

$$V = 2 C_L C_H L \quad (27)$$

where C_L is the lateral crack length, millimeter; C_H is the lateral crack depth, millimeter; L is the average trajectory length that an abrasive grain travels during effective cutting time Δt.

Transverse crack length can be obtained [22–24] as follows:

$$C_L = K_L \left(\frac{F_1}{K_C} \right)^{\frac{3}{4}} \quad (28)$$

Transverse crack depth can be obtained as follows:

$$C_H = K_H \left(\frac{F_1}{H} \right)^{\frac{1}{2}} \quad (29)$$

Where, F_1 is the contact force between single abrasive grain and workpiece; K_L is lateral crack length factor; K_H is lateral crack depth factor; H is material hardness, K_C is the fracture toughness expressed in stress intensity factor, MPa$\sqrt{\text{mm}}$; K_C can be calculated by:

$$K_C \cong \sqrt{2 \frac{E_f E_m}{E_m V_f + E_f V_m} \left(G_{cf} V_f + G_{cm} V_m \right)} \quad (30)$$

Where E_f and E_m are the elastic modulus of fiber and matrix material in CFRP, respectively. V_f and V_m are the volume fraction of the fiber and matrix in CFRP, respectively. G_{cf} and G_{cm} are fracture toughness values in elastic

energy release rate for fiber and matrix in the CFRP, respectively. The material removing volume of single abrasive grain can be obtained as follows:

$$V = 2\ K_{\mathrm{L}}K_{\mathrm{H}}\left(\frac{F_1}{K_{\mathrm{C}}}\right)^{\frac{3}{4}}\left(\frac{F_1}{H}\right)^{\frac{1}{2}} \int_0^{\Delta t}\sqrt{\left(v_{\mathrm{w}}-\frac{\pi}{30}n_{\mathrm{s}}\sin\frac{\pi}{30}n_{\mathrm{s}}t\right)^2+\left(\frac{\pi}{30}n_{\mathrm{s}}\bar{R}\cos\frac{\pi}{30}n_{\mathrm{s}}t\right)^2+(2\pi\mathrm{fA}\cos(2\pi\mathrm{ft}+\varphi_0))^2}dt \tag{31}$$

3.4 MRR and grinding force model

The material removal rate (MRR) of grinding unit is the summation of MRR of all abrasive grains on the end face of the cutting tool. So it can be obtained as follows:

$$MRR = nfV = 2\ nf\ K_{\mathrm{L}}K_{\mathrm{H}}\left(\frac{F_1}{K_{\mathrm{C}}}\right)^{\frac{3}{4}}\left(\frac{F_1}{H}\right)^{\frac{1}{2}} \int_0^{\Delta t}\sqrt{\left(v_{\mathrm{w}}-\frac{\pi}{30}n_{\mathrm{s}}\sin\frac{\pi}{30}n_{\mathrm{s}}t\right)^2+\left(\frac{\pi}{30}n_{\mathrm{s}}\bar{R}\cos\frac{\pi}{30}n_{\mathrm{s}}t\right)^2+(2\pi\mathrm{fA}\cos(2\pi\mathrm{ft}+\varphi_0))^2}dt \tag{32}$$

The material removal volume in unit time can be obtained as follows:

$$\mathrm{MRR} = 2a_{\mathrm{p}}Rv_{\mathrm{w}} \tag{33}$$

By solving both Eq. (32) and Eq. (33), it can be obtained as follows:

$$2\ a_{\mathrm{p}}R\ v_{\mathrm{w}} = 2\ nf\ K_{\mathrm{L}}K_{\mathrm{H}}\left(\frac{F_1}{K_{\mathrm{C}}}\right)^{\frac{3}{4}}\left(\frac{F_1}{H}\right)^{\frac{1}{2}} \int_0^{\Delta t}\sqrt{\left(v_{\mathrm{w}}-\frac{\pi}{30}n_{\mathrm{s}}\bar{R}\sin\frac{\pi}{30}n_{\mathrm{s}}t\right)^2+\left(\frac{\pi}{30}n_{\mathrm{s}}\cos\frac{\pi}{30}n_{\mathrm{s}}t\right)^2+(2\pi\mathrm{fA}\cos(2\pi\mathrm{ft}+\varphi_0))^2}dt \tag{34}$$

Through the indentation experiment of material to obtain the value of K_{L} and K_{H}, the grinding force can be defined by the following equations:

The grinding force of single grain can be obtained as follows:

$$F_1 = \sqrt[5]{K_{\mathrm{C}}^3H^2\left(\frac{2a_{\mathrm{p}}Rv_{\mathrm{w}}}{2nfK_{\mathrm{V}}\int_0^{\Delta t}\sqrt{\left(v_{\mathrm{w}}-\frac{\pi}{30}n_{\mathrm{s}}\bar{R}\sin\frac{\pi}{30}n_{\mathrm{s}}t\right)^2+\left(\frac{\pi}{30}n_{\mathrm{s}}\cos\frac{\pi}{30}n_{\mathrm{s}}t\right)^2+(2\pi\mathrm{fA}\cos(2\pi\mathrm{ft}+\varphi_0))^2}dt}\right)^4} \tag{35}$$

Where K_{V} is fracture volume factor ($K_{\mathrm{V}} = K_{\mathrm{L}}K_{\mathrm{H}}$) which is a proportionality parameter. It is assumed to be constant for a given workpiece material over a wide range of input variables. The value K_{V} can be obtained from the indentation experiments of material.

Hence, the relationship between grinding force and cutting parameters was expressed as:

$$F = n\sqrt[5]{K_{\mathrm{C}}^3H^2\left(\frac{2a_pRv_w}{2nfK_{\mathrm{V}}\int_0^{\Delta t}\sqrt{\left(v_{\mathrm{w}}-\frac{\pi}{30}n_{\mathrm{s}}\sin\frac{\pi}{30}n_{\mathrm{s}}t\right)^2+\left(\frac{\pi}{30}n_{\mathrm{s}}\bar{R}\cos\frac{\pi}{30}n_{\mathrm{s}}t\right)^2+(2\pi\mathrm{fA}\cos(2\pi\mathrm{ft}+\varphi_0))^2}dt}\right)^4} \tag{36}$$

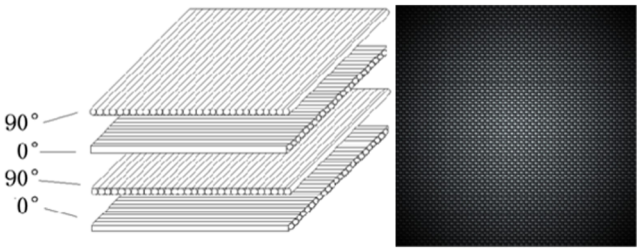

Fig. 5 Illustration of CFRP specimen

The grinding force calculated by Eqs. (19) and (36) is a mean value, which can reflect the average grinding force in unit volume material removal.

4 Design of experiments and experimental equipment

4.1 Workpiece material properties

The composite specimens were made of T300 carbon/epoxy unidirectional laminate with a ply thickness of in a cross-ply layup $[90/0]_s$, as illustrated in Fig. 5. The thickness of each carbon fiber yarn in the woven fabric is 0.263 mm. The CFRP plate contained 19 layers of fabric (38 layers of carbon fiber). Table 1 shows the material properties of CFRP. Dimensions of the CFRP plate used in the experiments were 20 mm × 5 mm × 5 mm. A dedicated fixture system was manufactured to attach the workpiece to a dynamometer. The composite specimen was held on the backing plate with two holes of 8 mm diameter located on one side. The CFRP specimen is attached to the backing plate with the help of paraffin wax.

Table 1 Material properties of CFRP

Material	Property	Unit	Value
CFRP	Density	g/cm^3	1.47
	Hardness	HRB	70–75
Carbon fiber	Density	g/cm^3	1.8
	Elastic modulus	GPa	230
	Axial tensile strength	GPa	4.9 or 5
	Poisson's ratio	–	0.3
	Fracture toughness	J/m^2	2
Epoxy matrix	Density	g/cm^3	1.2
	Elastic modulus	GPa	4.5
	Axial tensile strength	MPa	130
	Poisson's ratio	–	0.4
	Fracture toughness	J/m^2	500

4.2 Experimental set-up and conditions

The grinding experiments were conducted on a Haas DT-1 machining center with 11.2 kW spindle power and a maximum speed of 15,000 rpm. It is important to emphasize that the original spindle was replaced by a designed ultrasonic spindle system. The ultrasonic spindle system consists of a piezoelectric transducer, a collecting ring, a horn, and a diamond grinding unit. Ultrasonic vibration, defined as reciprocation harmonic motion with high frequency and low amplitude, is created by a piezoelectric transducer with input of sine voltage signal derive from an ultrasonic generator. Then the vibration amplitude is amplified by the horn, which is to attain desirable vibration amplitude values. A diamond grinding unit was mounted in the end of the horn, as shown in Fig. 6. Ultrasonic vibration of the workpiece with tunable amplitudes (from 0 to 0.01 mm) at frequency 20 kHz can be achieved by changing the input power.

The cutting tools used in experiments were electroplated diamond grinding units with different properties, as shown in Table 2. To verify that it is indeed independent of input variables (such as spindle speed, cutting depth, feed rate, and grit size (mesh #)), a series of experiments with different input variables were designed. The design of experiments is given in Table 3.

The grinding dynamometer (Model 9257B, Kistler Inc., Winterthur, Switzerland) was used to measure the cutting force (F) in the axial direction. Specifically, the electrical signals from the dynamometer were amplified by the multichannel charge amplifier (Model 5080, Kistler Inc.,

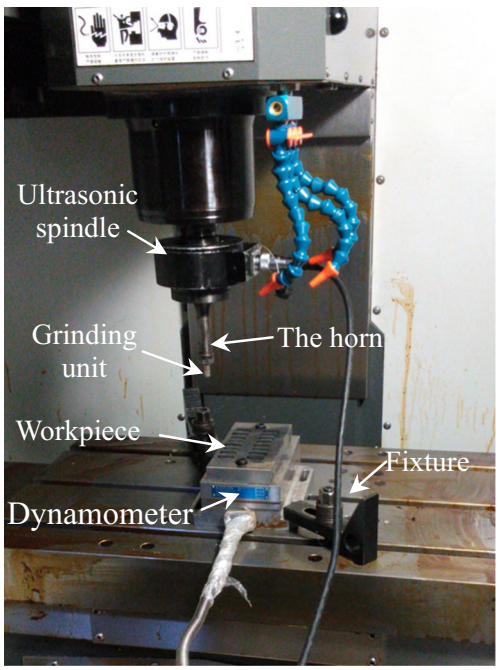

Fig. 6 Experimental set-up

Table 2 Material properties of the grinding unit

Tool no.	Grit size (mesh #)	Diameter of the tool handle	Abrasive size r (μm)	Concentration	Wheel diameter D (mm)	Total length (mm)
1	60#	6	88	100	8	45
2	100#	6	41	100	8	45
3	120#	6	30	100	8	45
4	150#	6	40	100	8	45
2	200#	6	20	100	8	45

Winterthur, Switzerland) and then transformed into digital signals by the A/D converter. After being processed by a signal conditioner, the digital signals were collected by the data acquisition system (DEWE soft, Austria). The recorded data were downloaded onto a personal computer. The sampling frequency was 20 kHz. The average value of the cutting force, which is the mean value of the entire cutting force curve, was chosen to represent the cutting force.

4.3 Measurement procedures for output variables

A laser Doppler vibrometer (Model LV-S01-ST, Sunny Instruments Singapore Pte. Ltd., Singapore) was used to measure the vibration amplitude of the ultrasonic spindle system. A data acquisition and analysis system software (Model quicksa, Sunny Instruments Singapore Pte. Ltd., Singapore) was dedicated to the acquisition and processing of vibration measurement data. It was used to measure data into real-time collection and storage and to analyze and save the data by recording to the computer.

5 Results and discussion

Investigations were carried out into the comparison of common grinding with ultrasonic vibration assisted grinding. The effects of input variables on grinding force were studied. All of the experiments with a total of 40 tests were divided into four groups with different input variables.

5.1 Effects of spindle speed on cutting force

Figure 7 shows influences of spindle speed on cutting force. It is obvious that the grinding force in RUFG is smaller than conventional grinding (CG). If the other input variables (such as cutting depth, feed rate, and grit size) do not change, with the spindle speed increases, according to Eq. (33), the material removal volume processed by one abrasive grain during a single vibration cycle does not change. However, the trajectory length of single grain contact with material in single rotation period has increased. From Eq. (36), it can be obtained that grinding force will decrease. In the CG process, as the spindle speed increases, the reduction of the cutting force trends quickly and, in RUFG process, as the spindle speed increases, cutting force reduce speed is relatively slow.

5.2 Effects of cutting depth on cutting force

Figure 8 shows influences of cutting depth on cutting force. If the other input variables (such as spindle speed, feed rate, and grit size) do not change, as the cutting depth increases, according to Eq. (33), the material removal volume processed by one abrasive grain during a single vibration cycle will increase. However, the trajectory length of single grain contact with material in single rotation period does not change. From Eq. (36), it can be obtained that grinding force will increase.

Table 3 Experimental conditions for RUFG

Experiment	Spindle speed (rpm)	Cutting depth (mm)	Feed rate (mm/min)	Grit size (mesh #)	Wheel diameter D (mm)	Ultrasonic amplitude (mm)
1st group	500, 1000, 1500, 2000, 2500	0.15	180	100	8	0, 0.01
2nd group	1500	0.05, 0.1, 0.15, 0.2, 0.25	180	100	8	0, 0.01
3rd group	1500	0.15	60, 120, 180, 240, 300	100	8	0, 0.01
4th group	1500	0.15	180	60, 100, 120, 150, 200	8	0, 0.01

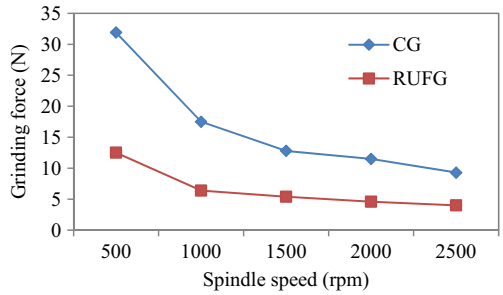

Fig. 7 Relationship between grinding force and spindle speed

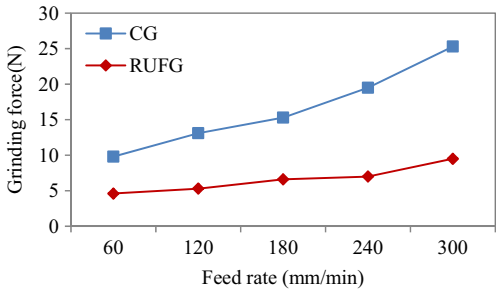

Fig. 9 Relationship between grinding force and feed rate

Compared with the spindle speed, the cutting depth has less influence on the cutting force.

5.3 Effects of feed rate on cutting force

Figure 9 shows influences of feed rate on cutting force. The grinding force in RUFG is also smaller than CG. Compared with the cutting depth, feed rate has similar effects on the cutting force; as the feed rate increases, according to Eq. (33), the material removal volume processed by one abrasive grain during a single vibration cycle will increase, but the trajectory length of single grain contact with material in single rotation period do not change. From Eq. (36), it can be obtained that grinding force will increase.

5.4 Effects of grit size on cutting force

Figure 10 shows influences of grit size on cutting force. If grit size increases, the abrasive size decreases. According to Eq. (14), the indentation depth of abrasive grain will increase; increase in indentation depth leads to increase in the effective cutting time Δt and decrease in maximum impact force. The decreasing rate in maximum impact force is higher than the increasing rate in effective cutting time. If abrasive size decreases while the other input variables keep unchanged, grinding force will decrease.

However, if grit size increases, number of active abrasive grains increases. According to Eq. (14), the indentation depth of abrasive grain will decrease; decrease in indentation depth leads to decrease in the effective cutting time Δt and increase in maximum impact force. The increasing rate in number of active abrasive grains is higher than the decreasing rate in effective cutting time. If number of active abrasive grains increases while the other input variables keep unchanged, grinding force will increase. In conclusion, if grit size increases, grinding force will remain substantially unchanged.

6 Conclusions

In this paper, a method for improving the performance of RUFG for CFRP material processing is presented. The experimental RUFG was carried out, and the results were analyzed and discussed. The trends of predicted effects of input variables on cutting force agree well with the trends determined experimentally. The following conclusions are drawn from this study:

1) The average values of grinding force during RUFG process are smaller than those of CG.
2) Grinding force will decrease as the spindle speed increases. In the CG process, as the spindle speed increases the reduction of the cutting force trends quickly, but, in RUFG process, as the spindle speed increases cutting force reduce speed is relatively slow.
3) Grinding force will increase as cutting depth and feed rate increase.
4) Grinding force will remain substantially unchanged as grit size increases, because if grit size increases, the abrasive size decreases and number of active abrasive grains increases, which cause little change in grinding force.

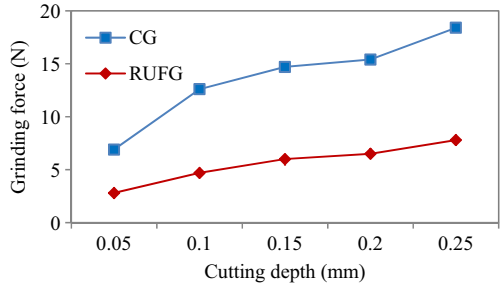

Fig. 8 Relationship between grinding force and cutting depth

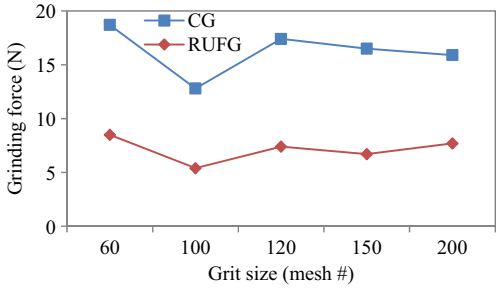

Fig. 10 Relationship between grinding force and grit size

Acknowledgments The authors would like to thank the Science and Technology Department of Hubei Province (Grant Number 2015BAA022) and the State Key Lab of Digital Manufacturing Equipment and Technology (Grant Number DMETKF2015014) for funding this study.

References

1. Rahamathullah I, Shunmugam M (2014) Mechanistic approach for prediction of forces in micro-drilling of plain and glass reinforced epoxy sheets. Int J Adv Manuf Technol 75(5–8):1177–1187
2. Soutis C (2005) Fibre reinforced composite in aircraft construction. Prog Aerosp Sci 41:143–151
3. Li H, Qin X, He G, Jin Y, Sun D, Price M (2016) Investigation of chip formation and fracture toughness in orthogonal cutting of UD-CFRP. Int J Adv Manuf Technol 82:1079–1088
4. Liu D, Tang Y, Cong WL (2012) A review of mechanical drilling for composite laminates. Compos Struct 94:1265–1279
5. Zenia S, Ben Ayed L, Nouari M, Delamézière A (2015) Numerical analysis of the interaction between the cutting forces, induced cutting damage, and machining parameters of CFRP composites. Int J Adv Manuf Technol 78:465–480
6. Liu J, Chen G, Ji C, Qin X, Li H, Ren C (2014) An investigation of workpiece temperature variation of helical milling for carbon fiber reinforced plastics (CFRP). Int J Mach Tools Manuf 86:89–103
7. Ishida T, Noma K, Kakinuma Y, Aoyama T, Hamada S, Ogawa H, Higaino T (2014) Helical milling of carbon fiber reinforced plastics using ultrasonic vibration and liquid nitrogen. Procedia CIRP 24: 13–18
8. Li ZC, Jiao Y, Deines TW, Pei ZJ, Treadwell C (2005) Rotary ultrasonic machining of ceramic matrix composites: feasibility study and designed experiments. Int J Mach Tools Manuf 45: 1402–1411
9. Ning FD, Cong WL, Pei ZJ, Treadwell C (2016) Rotary ultrasonic machining of CFRP: a comparison with grinding. Ultrasonics 66: 125–132
10. Wang X, Zhou M, Gan GK, Ngoi B (2002) Theoretical and experimental studies of ultraprecision machining of brittle materials with ultrasonic vibration. Int J Adv Manuf Technol 20(2):99–102
11. Liu JW, Baek DK, Ko TJ (2014) Chipping minimization in drilling ceramic materials with rotary ultrasonic machining. Int J Adv Manuf Technol 72:1527–1535
12. Qin N, Pei ZJ, Treadwell C, Guo DM (2009) Physics-based predictive cutting force model in ultrasonic-vibration-assisted grinding for titanium drilling. J Manuf Sci Eng ASME 131(4):481–498
13. Liu D, Cong WL, Pei ZJ, Tang Y (2012) A cutting force model for rotary ultrasonic machining of brittle materials. Int J Mach Tools Manuf 52:77–84
14. Cong WL, Pei ZJ, Sun X, Zhang CL (2014) Rotary ultrasonic machining of CFRP: a mechanistic predictive model for cutting force. Ultrasonics 54:663–675
15. Wang Y, Lin B, Wang S, Cao X (2014) Study on the system matching of ultrasonic vibration assisted grinding for hard and brittle materials processing. Int J Mach Tools Manuf 77:66–73
16. NS H, Zhang LC (2004) Some observations in grinding unidirectional carbon fibre-reinforced plastics. J Mater Process Technol 152:333–338
17. NS H, Zhang LC (2003) A study on the grindability of multidirectional carbon fibre-reinforced plastics. J Mater Process Technol 140:152–156
18. Pei ZJ, Prabhakar D, Ferreira PM, Haselkorn M (1995) A mechanistic approach to the prediction of material removal rates in rotary ultrasonic machining. J Eng Ind 117(2):142–151
19. Kaw AK (2006) Chapter 3 micromechanical analysis of a lamina, mechanics of composite materials, second edn. CRC Press, Boca Raton
20. Zhang C, Zhang J, Feng P (2013) Mathematical model for cutting force in rotary ultrasonic face milling of brittle materials. Int J Adv Manuf Technol 69:161–170
21. Gong H, Fang FZ, Hu XT (2010) Kinematic view of tool life in rotary ultrasonic side milling of hard and brittle materials. Int J Mach Tools Manuf 50:303–307
22. Lawn BR, Evans AG, Marshall DB (1980) Elastic/plastic indentation damage in ceramics: the median/radial crack system. J Am Ceram Soc 63(9–10):574–581
23. Marshall DB, Lawn BR, Evans AG (1982) Elastic/plastic indentation damage in ceramics: the lateral crack system. J Am Ceram Soc 65(11):561–566
24. Collins JA (1981) Failure of materials in mechanical design. Wiley, New York